Journal of Geophysical Research: Atmospheres

RESEARCH ARTICLE
10.1029/2017JD028076

Direct Measurements of Momentum Flux and Dissipative Heating in the Surface Layer of Tropical Cyclones During Landfalls

Jie Ming[1,2] **and Jun A. Zhang**[3,4]

[1]Key Laboratory of Mesoscale Severe Weather/MOE and School of Atmospheric Sciences, Nanjing University, Nanjing, China, [2]Joint Center for Atmospheric Radar Research of Centre of Modern Analysis/Nanjing University (CMA/NJU), Nanjing, China, [3]Hurricane Research Division, Atlantic Oceanographic and Meteorological Laboratory, National Oceanographic and Atmospheric Administration, Miami, FL, USA, [4]Cooperative Institute for Marine and Atmospheric Studies, University of Miami, Miami, FL, USA

Key Points:
- Direct measurements of momentum flux, drag coefficient, and TKE are substantially larger in coastal regions with larger surface roughness
- Dissipative heating (DH) estimated using the theoretical method is generally larger than that estimated using the spectra method
- The overestimation of DH by the theoretical method is much smaller over the coastal land than over the shallow water at a given wind speed

Correspondence to:
J. Ming and J. A. Zhang,
jming@nju.edu.cn;
jun.zhang@noaa.gov

Citation:
Ming, J., & Zhang, J. A. (2018). Direct measurements of momentum flux and dissipative heating in the surface layer of tropical cyclones during landfalls. *Journal of Geophysical Research: Atmospheres*, *123*, 4926–4938. https://doi.org/10.1029/2017JD028076

Received 20 NOV 2017
Accepted 22 APR 2018
Accepted article online 1 MAY 2018
Published online 17 MAY 2018

Abstract This study analyzes high-frequency wind data collected by research towers in the surface layer of Typhoons Hagupit (2008) and Chanthu (2010) to investigate the characteristics of the momentum flux, turbulent kinetic energy (TKE), drag coefficient, and dissipative heating (DH) during landfalls. It is found that the momentum flux TKE and DH increase with the wind speed up to the maximum observed wind speed (~40 m/s), in agreement with previous studies that presented eddy correlation flux data in a similar condition but with lower maximum observed wind speed. However, the momentum flux, TKE, drag coefficient, and DH are found to be substantially larger in Typhoon Chanthu (2010) than those in Typhoon Hagupit (2008) at a given wind speed, likely due to much rougher surface conditions surrounding the tower deployed in Typhoon Chanthu (2010). Furthermore, the DH is calculated using two different methods: (1) based on surface-layer theory and (2) based on the standard turbulent spectra method. It is found that the first method tends to overestimate the value of DH compared to the second method, and the overestimation of the DH by the first method is much smaller over rougher underlying surface than over the smoother underlying surface. Our analysis shows that the magnitude of the DH over land is as large as the sensible heat flux (~100 W/m^2) previously observed over the ocean, which should not be neglected in numerical models simulating tropical cyclones during landfalls.

1. Introduction

It is well known that physical processes tied to turbulent transport in the planetary boundary layer (PBL) play a significant role in the lifecycle of a tropical cyclone (TC; e.g., Bryan, 2012; Davis et al., 2008; Ooyama, 1969; Wroe & Barnes, 2003; Zhang, Marks, et al., 2011). Malkus and Riehl (1960) found that the heat transfer from the ocean to the atmosphere determines the intensity and structure of a TC, especially the eyewall structure. Emanuel (1986, 1995) pointed out that the air-sea exchange of momentum and enthalpy fluxes are responsible for the intensification of a TC and its maximum potential intensity (MPI). Several previous numerical studies demonstrated that the intensity and structure of TCs are sensitive to the parameterized turbulent fluxes in the PBL schemes in various numerical models (Braun & Tao, 2000; Bryan, 2012; Green & Zhang, 2014; Kepert, 2012; Ming & Zhang, 2016; Nolan et al., 2009; Ooyama, 1969; Smith & Thomsen, 2010).

Besides turbulent fluxes, another important physical parameter in the surface layer of TC is dissipative heating (DH). The DH is induced by frictional dissipation of kinetic energy through molecular processes. It is an important thermodynamic energy source for TCs and one of the key factors in the MPI theory. The DH was first studied by Bister and Emanuel (1998) using both a simple balance model and an axisymmetric nonhydrostatic model in idealized simulations of TCs. They demonstrated that the maximum surface wind speed increases by ~ 20 m/s and the central minimum sea level pressure decreases by ~40 hPa when the DH was included in their simulations. They suggested that the DH should be included in numerical models for TC simulations and forecasts. Note that a theoretical study given by Kieu (2015) discussed the limitation of including the DH in the MPI theory proposed by Bister and Emanuel (1998) through a detailed energy budget analysis. Businger and Businger (2001) investigated the DH estimated from the turbulent kinetic energy (TKE) budget equation and also suggested that the DH should be included in numerical models, particularly in models resolving mesoscale structures of TCs.

Furthermore, there were several numerical studies that investigated the effect of DH on the intensity and structure of TCs. Zhang and Altshuler (1999) used three-dimensional, nonhydrostatic cloud-resolving model with explicit simulations of Hurricane Andrew (1992) to examine the influence of DH on Andrew's intensity and structure. They concluded that the central pressure was 5–7 hPa lower and the maximum surface wind speed was 10% higher in the simulations with the DH than those in the simulations without the DH. They also showed that DH tends to increase the sensible heat flux at the top of the surface layer, leading to a warmer surface layer. The net heating rate in their control simulation was 30%–40% lower than that in the simulation including DH. Wang (2001) included the DH in his triply nested movable mesh primitive equation model (TCM3) through a TKE term. Based on the dissipation of the TKE, the DH effect was also implemented into the operational Geophysical Fluid Dynamics Laboratory (GFDL) model in 2001 (Bender et al., 2007). Jin et al. (2007) used the U.S. Navy's operational mesoscale model (the Coupled Ocean/Atmosphere Mesoscale Prediction System) to investigate the impact of DH on TC intensity forecasts. They found that the intensity forecast was improved by 10%–20% with the DH included in their simulations of 10 TCs, but they found little effect of DH on the track forecast. Zeng et al. (2010) used a newly developed, fully compressible, nonhydrostatic primitive equation model (TCM4) to compare TC simulations with and without DH. They found that the maximum surface wind speed increased by 10.5% and the minimum sea surface pressure decreased by 8.1 hPa when including the DH in their idealized simulations. Cheng et al. (2012) examined effects of DH on structure and intensity of a real TC using the fifth-generation Pennsylvania State University–National Center for Atmospheric Research Mesoscale Model (MM5). They concluded that the DH could warm the lower atmosphere within the high-wind region, because the heating offsets the cooling induced by the evaporation of sea spray.

However, there were few observational studies estimating the magnitude of the DH in boundary layer of TCs. Zhang (2010) was the first study that has examined the DH using observational data in TCs. Two different methods were used by Zhang (2010) to compute the DH with the fast-response wind data collected in the boundary layer of five Atlantic hurricanes. They pointed out that the method of multiplying the drag coefficient by the cubic of the surface wind speed as used by Bister and Emanuel (1998) overestimated the DH compared to the method in which the DH was calculated by integrating the rate of dissipation in the surface layer. Zhang, Zhu, et al. (2011) examined the calculation of DH using the same two methods using high-frequency wind data of three landfalling hurricanes. Their results were consistent with the finding of Zhang (2010) over the ocean. Till now, few studies have investigated the DH using the observed data over the Western Pacific basin. The present study aims to fill this gap by analyzing the high-frequency wind data to assess turbulent characteristics of landfalling typhoons over the Western Pacific Ocean. The objective of this paper is to compare the momentum flux, drag coefficient, TKE, and DH measured over different underlying surfaces during TC landfalls.

2. Data and Methodology

In this study, the high-frequency wind data were collected by two research towers during the passage of two typhoons, each in Typhoons Hagupit (2008) and Chanthu (2010). The tower deployed in Typhoon Hagupit (2008) is referred to as Tower1 and the tower deployed in Typhoon Chanthu (2010) is referred to as Tower2, hereafter. The locations of the two towers relative to the storm tracks are plotted in Figures 1a and 1c. The observational period in Typhoon Hagupit (2008) was from 1400 UTC 23 September to 0500 UTC 24 September 2008. In Typhoon Chanthu (2010), the observational period was from 2100 UTC 21 July to 1100 UTC 22 July 2010. Tower1 was located at 111.374°E, 21.439°N on the Zhizai Island which is separated from the main land and is surrounded by shallow water. The area of the Zhizai Island is about 3,000 m^2 and the surface is covered by sand and weeds (Figure 1b). Tower2 was located at 110.506°E, 20.975°N on the Donghai Island which is 2.3 km inland from the coast line. Tower2 was surrounded by farmland, woodland, and residential areas (Figure 1d).

A brief summary of the life cycle of the two typhoons is given below. Typhoon Hagupit (2008) formed as a tropical depression over northeast of Guam on 19 September 2008. It intensified into a typhoon on 20 September 2008 and turned to northwestward after that. At 2245 UTC, on 23 September 2008, Typhoon Hagupit made landfall at Dianbai Town of Maoming City in Guangdong Province of China with the minimum sea level pressure of 940 hPa and the maximum surface wind speed of 110 kts based on the best track from

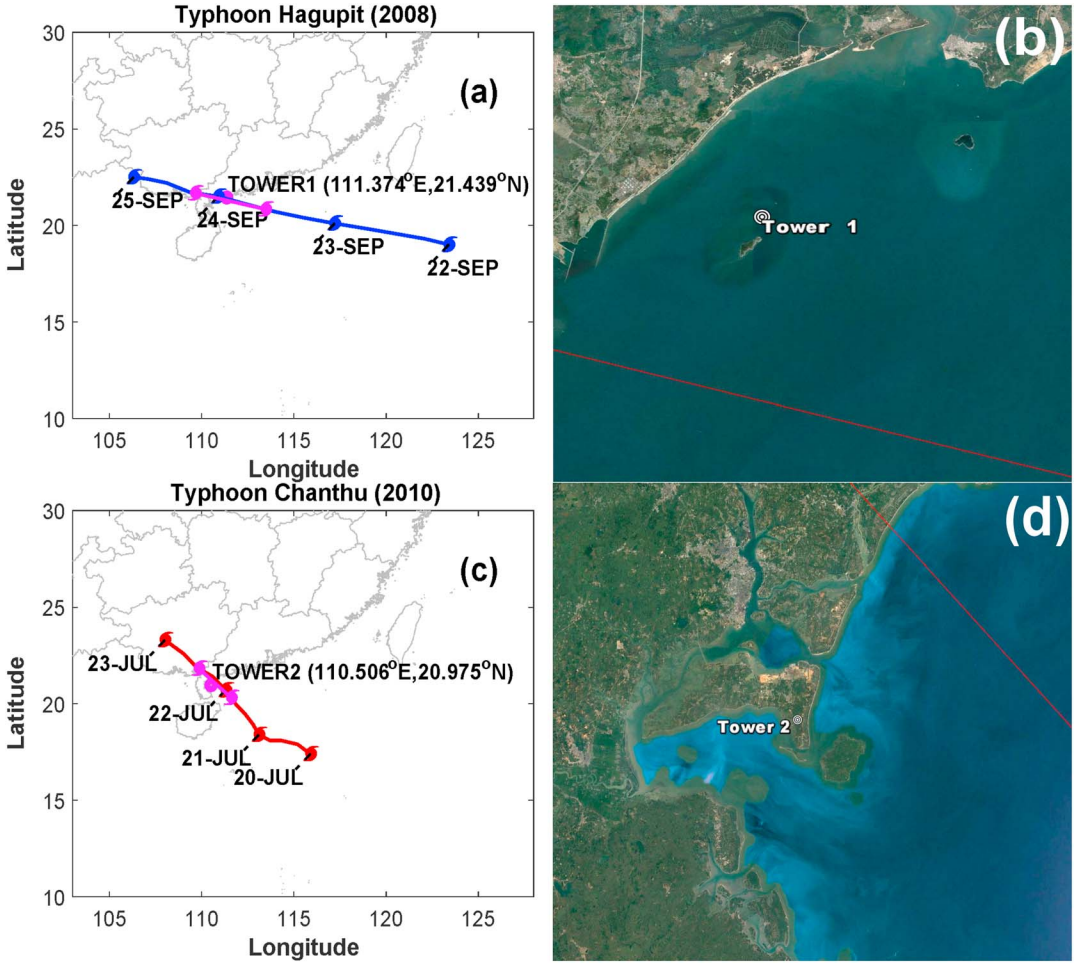

Figure 1. (a) Plot of the location of Tower1 with the track of Typhoon Hagupit (2008). (b) Plot of the surface topography around Tower1. (c) Plot of the location of Tower2 with the track of Typhoon Chanthu (2010). (d) Plot of the surface topography around Tower2. The magenta color stands for the period we focused on.

the Joint Typhoon Warning Center (JTWC; Figure 2a). The center of Typhoon Hagupit (2008) was 8.5 km away from the Zhizai Island where Tower1 was deployed. Typhoon Chanthu (2010) originated from a tropical depression over the South China Sea on 18 July 2010. The storm intensified to typhoon intensity by 1800 UTC, 21 July. At 0545 UTC, on 22 July 2010, Typhoon Chanthu made landfall at the Wuchuan city in

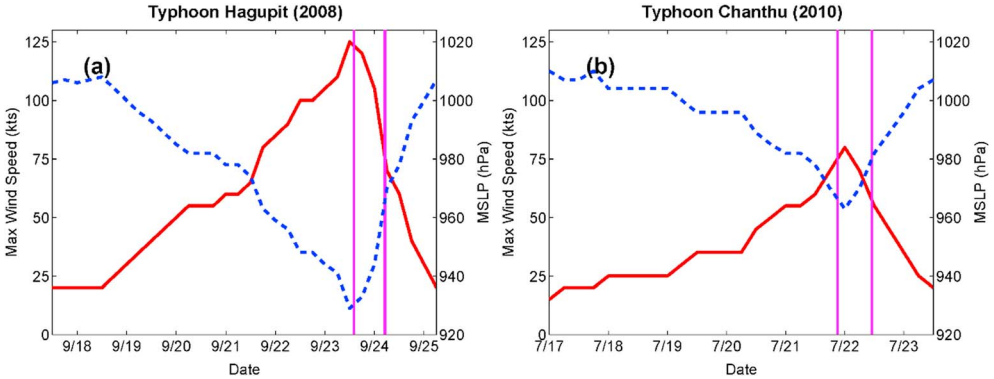

Figure 2. Observed minimum sea level pressure (blue dashed line, unit: hPa) and maximum surface wind speed (red solid line, unit: kts) of Typhoons (a) Hagupit (2008) and (b) Chanthu (2010) from Joint Typhoon Warning Center. The two magenta lines cover the periods of interest for data analysis.

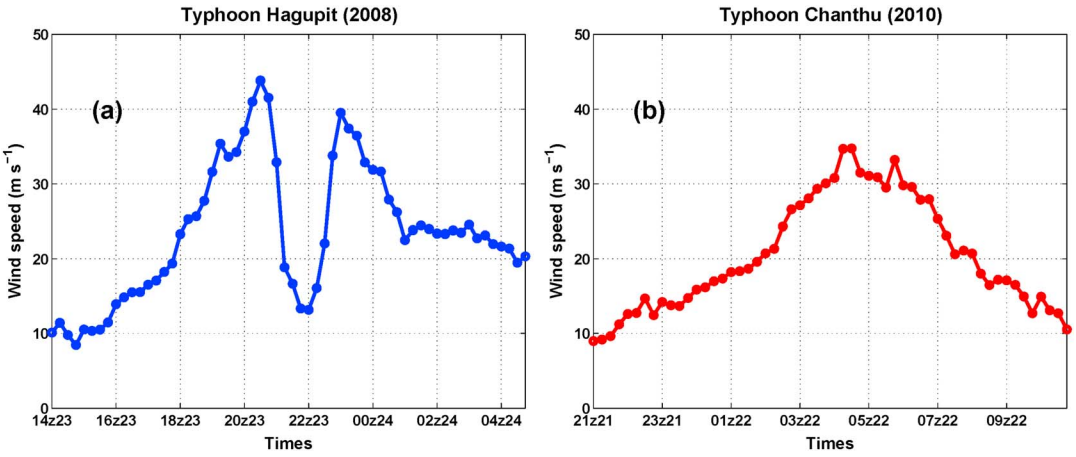

Figure 3. Plot of the 15-min averages of the wind speed in (a) Typhoon Hagupit (2008) from 1400 UTC 23 September to 0500 UTC 24 September 2008 (blue, unit: m/s), and (b) Typhoon Chanthu (2010) from 2100 UTC 21 July to 1100 UTC 22 July 2010 (red, unit: m/s).

Guangdong Province of China. The maximum surface wind speed from the best track is 80 kts and the minimum sea level pressure is 963 hPa before landfall (Figure 2b).

Both towers are 100 m high with the Gill Windmaster Pro ultrasonic anemometers installed at 60 m on Tower1 and 70 m on Tower2. The sampling frequency of the measured three-dimensional wind speed is 10 Hz. The 15-min averaged wind speed during the periods of observations in the two typhoons are plotted in Figure 3. When Typhoon Hagupit (2008) passed Tower1, its storm center was close to the tower, as indicated by the time series of the mean wind speed showing a nice "M" shape wind profile (Figure 3a). The observed maximum wind speed reached 43.8 m/s in Typhoon Hagupit, which is much higher than that shown in previous studies (Zhang, Zhu, et al., 2011). Tower2 was located on the left side of Typhoon Chanthu (2010) such that the time series of the wind speed shows a weak increase and decrease trend before and after Typhoon passed Tower2. The maximum wind speed measured during the passage of Typhoon Chanthu (2010) was ~36 m/s (Figure 3b).

The high-frequency data of wind speed was processed using the same procedures as detailed by Ming et al. (2014). The quality of the three-dimensional wind speed is controlled by the spectral analysis before the flux calculation following Zhang et al. (2009). As an example, the spectra of the three-component wind velocities from a good flux run, each from the two typhoons, are plotted in Figure 4. The −5/3 slope seen in the log-log scale plot of the spectra as a function of frequency confirms the Kolmogorov's power law, which also confirms the good quality of the wind data as the inertial subrange at high frequency can be resolved. The cospectra and cumulative summations of cospectra of the momentum flux from the same flux runs as in Figure 4 are plotted in Figure 5. For a good flux run, the cumulative summation of cospectra approaches asymptotically to a constant value in both the high and low ends of the frequency band and varies continuously in between, indicating stationarity. The flatness of the cumulative summations of cospectra at low- and high-frequency regions indicates that the energy of the example period is well contained from 0.001 to 1 Hz (Figures 5c and 5d). Based on the spectra analysis, a total of 83 good flux runs are identified to calculate the momentum flux, turbulent kinetic energy (TKE), roughness length, drag coefficient, and DH that are defined below.

Based on the eddy correlation method, the flux of momentum is defined by

$$\vec{\tau} = -\rho\left(\overline{u'w'}\ \vec{i} + \overline{v'w'}\ \vec{i}\right) \tag{1}$$

where u, v, w, and ρ represent longitudinal, lateral, vertical components of wind speed and the air density. The prime represents the turbulent fluctuation and overbar is time averaging over 15 min.

Using the turbulent fluctuations, the TKE (e) is in the form of

$$e = \frac{1}{2}\left(\overline{u'^2} + \overline{v'^2} + \overline{w'^2}\right) \tag{2}$$

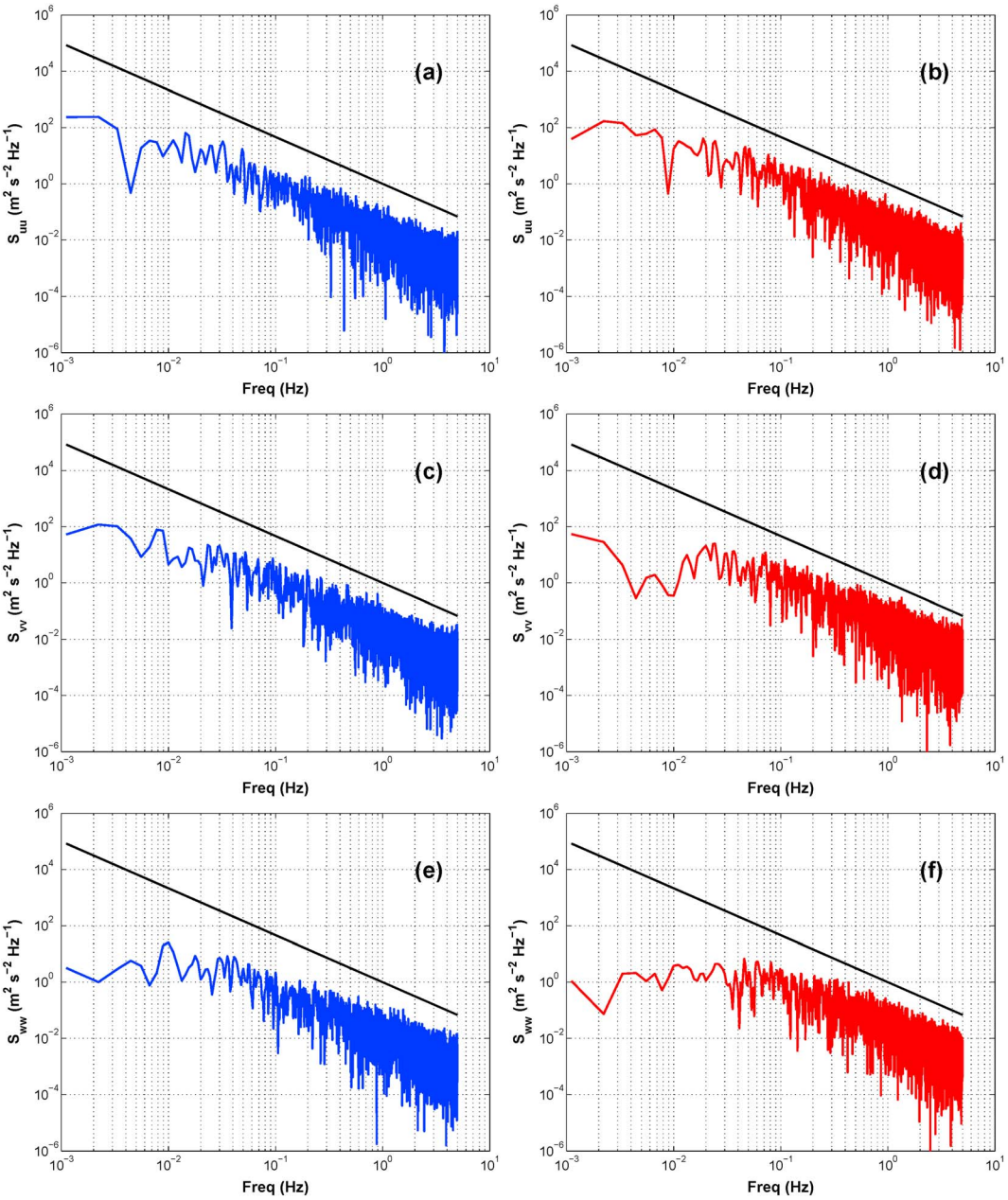

Figure 4. Plots of the power spectra for the three components of wind velocities from two typical good flux runs, each in Typhoons Hagupit (2008) and Chanthu (2010). The blue colors are from Typhoon Hagupit (2008) and the red colors are from Typhoon Chanthu (2010). The black lines stand for the −5/3 slope.

The momentum flux in the surface layer can also be described in terms of exchange coefficient as follows:

$$\tau = \rho u_*^2 = \rho C_D U^2 \tag{3}$$

where u_* is the friction velocity, U is the horizontal wind speed at the observed height, and C_D is the drag coefficient. The u_* is define as

$$u_* = \left(\frac{|\tau|}{\rho}\right)^{\frac{1}{2}} \tag{4}$$

The U is in the form of:

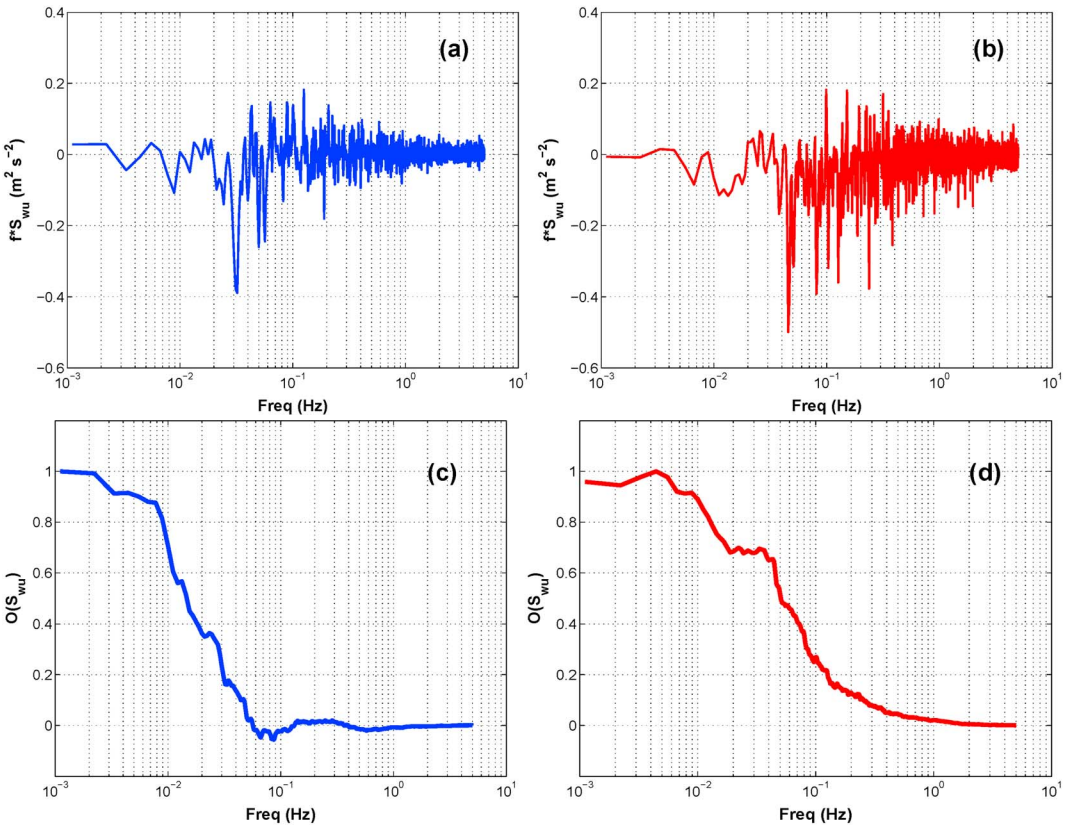

Figure 5. Plots of the cospectra and cumulative summations of cospectra of along-wind momentum flux from two typical good flux runs, each in Typhoons Hagupit (2008) and Chanthu (2010). The blue colors are from typhoon Hagupit (2008) and the red colors are from typhoon Chanthu (2010).

$$U(z) = \left(\frac{u^*}{k}\right) \ln\left(\frac{z}{z_0}\right) \tag{5}$$

where k is a constant and equal to 0.4, z is the height of the observed horizontal wind speed, and z_0 is the roughness length.

The z_0 is calculated as follows:

$$z_0 = ze^{\left(-\frac{kU}{u_*}\right)} \tag{6}$$

Furthermore, C_D is calculated as follows:

$$C_D = \frac{u_*^2}{U^2} \tag{7}$$

Following Zhang (2010) and Zhang, Zhu, et al. (2011), the DH can be calculated using the same method as in Bister and Emanuel (1998), which is referred as the BE method hereafter:

$$DH = \rho C_D U^3 \tag{8}$$

where ρ is the air density, C_D is the drag coefficient, and U is the horizontal wind speed at the observed height.

Also, the DH can directly measure by integrating the dissipation rate in the surface layer, and the formula is

$$\mathrm{DH} = \rho \int_0^z \varepsilon \mathrm{d}z = \rho \bar{\varepsilon} z \tag{9}$$

where z is the surface layer depth and we use the observed height here following Zhang (2010) assuming the flux is a constant in the surface layer according to the Monion-Obukhov similarity theory; the overbar represents the mean value over the surface layer; ε is the dissipation rate and is given by

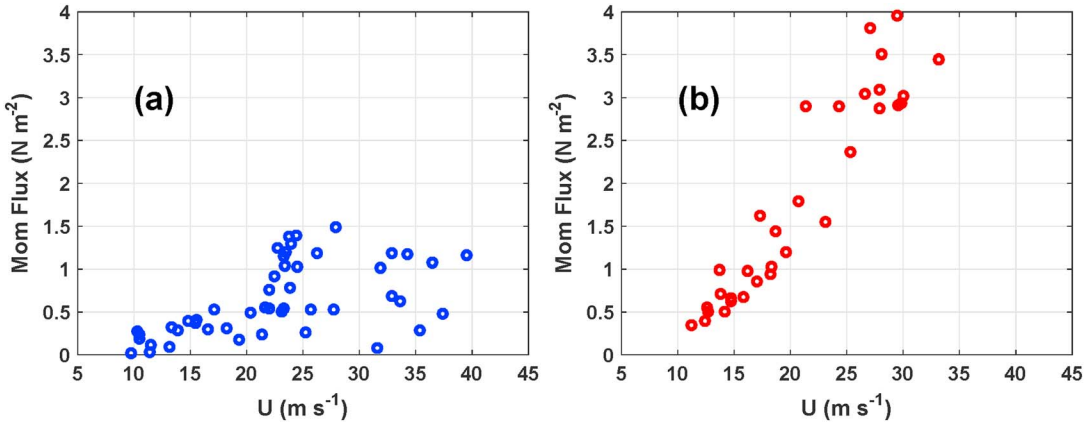

Figure 6. Plots of the momentum flux as function of the mean wind speed for each flux run in (a) Typhoon Hagupit (2008, blue) and (b) Typhoon Chanthu (2010, red).

$$\varepsilon = \alpha_u^{-\frac{3}{2}} \frac{2\pi f}{U} [f S_{uu}(f)]^{\frac{3}{2}} \tag{10}$$

Where $\alpha_u$is the one-dimensional Kolmogorov constant and equals to 0.5 (Sreenivasan, 1995), f is the frequency, U is the mean wind speed, and S_{uu} is the power spectral density of longitudinal wind speed. The DH calculated using the combination of equations (9) and (10) is based on the turbulent spectra, thus is referred to as turbulent spectra method hereafter. Note that the main difference of these two methods for estimating the DH is that the BE method assumes that all the kinetic energy due to friction is converted to heat, while the spectra method gives the direct measurement of DH based on the nature of turbulent flow. As pointed out by Zhang (2010) and Zhang, Zhu, et al. (2011), the BE method derived from the simplified TKE budget may overestimate the DH when the shear production is balanced by the dissipation term. They also pointed out the possible influence of surface waves on the energy dissipation over the ocean.

3. Results

The momentum flux is plotted against the observed mean wind speed in Figure 6 for all the good flux runs in both typhoons. In Typhoon Hagupit (2008), when the mean wind speed is $<$25 m/s, the momentum flux increases with the mean wind speed, but the momentum flux tends to level off when the mean wind speed is $>$25 m/s (Figure 6a). On the other hand, in Typhoon Chanthu (2010), the momentum flux continues to increase with the wind speed even when the mean wind speed is $>$25 m/s (Figure 6b). At a given wind speed, the magnitude of the momentum flux in Typhoon Chanthu (2010) is much larger than that in Typhoon Hagupit (2008). In addition, the momentum flux increases slower with the wind speed in Typhoon Hagupit

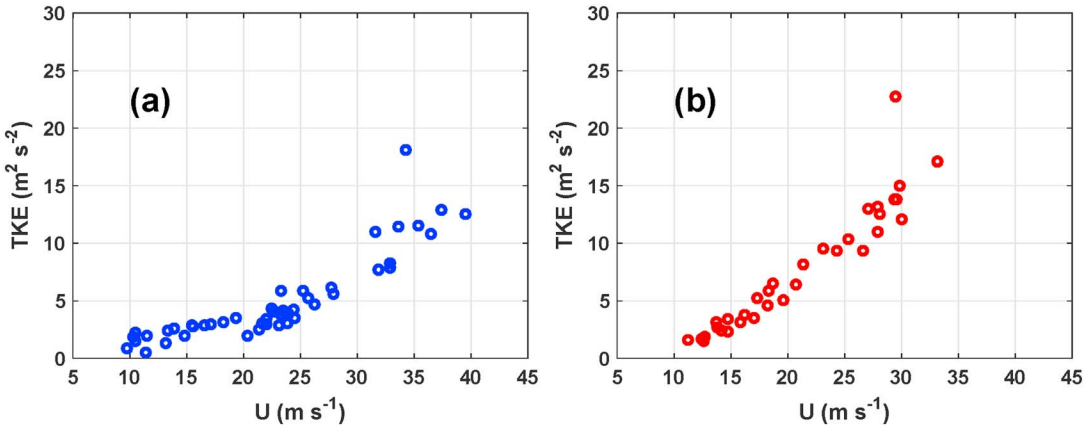

Figure 7. Plots of the TKE as function of the mean wind speed for each flux run in (a) Typhoon Hagupit (2008, blue) and (b) Typhoon Chanthu (2010, red).

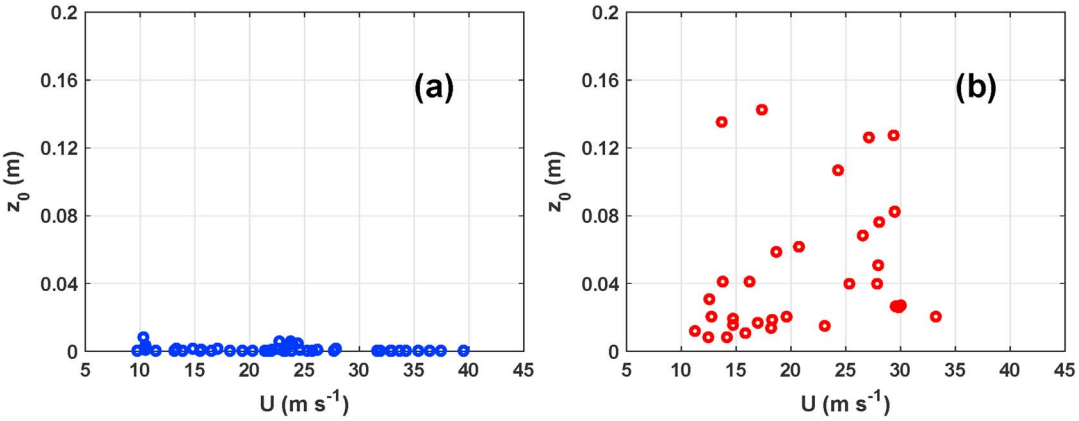

Figure 8. Plots of the roughness length as function of the mean wind speed for each flux run in (a) Typhoon Hagupit (2008, blue) and (b) Typhoon Chanthu (2010, red).

(2008) than in Typhoon Chanthu (2010) when the mean wind speed is $<$25 m/s. This difference in the magnitude of momentum flux can be attributed to the surface roughness difference between Tower1 and Tower2.

Interestingly, the behavior of the TKE in relation to the wind speed is different from that of the momentum flux, in that the TKE continuously increases with the mean wind speed in both typhoons (Figure 7). Similar to the momentum flux, the TKE in Typhoon Hagupit (2008) increases slower with the wind speed than in Typhoon Chanthu (2010).

The roughness length (z_0) calculated based on equation (6) is plotted against the wind speed in Figure 8 for the two typhoons. As mentioned earlier, Tower1 in Typhoon Hagupit (2008) is located on a small island named Zhizai Island, where the upstream topography is close to that over shallow water, while Tower2 in Typhoon Chanthu (2010) is located on the Donghai Island, which is connected to the main land and is surrounded by farmlands. It is evident from Figure 8 that the difference in the roughness length computed based directly on measured momentum flux and wind speed is consistent with that based on surface land types. Values of z_0 range from 2 to 15 cm for Tower2, which is an order of magnitude larger than that for Tower1.

The drag coefficient (C_D) is presented as a function of the wind speed in Figures 9a and 9b for Typhoons Hagupit (2008) and Chanthu (2010), respectively. It is evident that the magnitude of C_D in Typhoon Chanthu (2010) is much larger than that in Typhoon Hagupit (2008). The difference in the behavior of the drag coefficient between Tower1 and Tower2 observations is believed to be related to the difference in

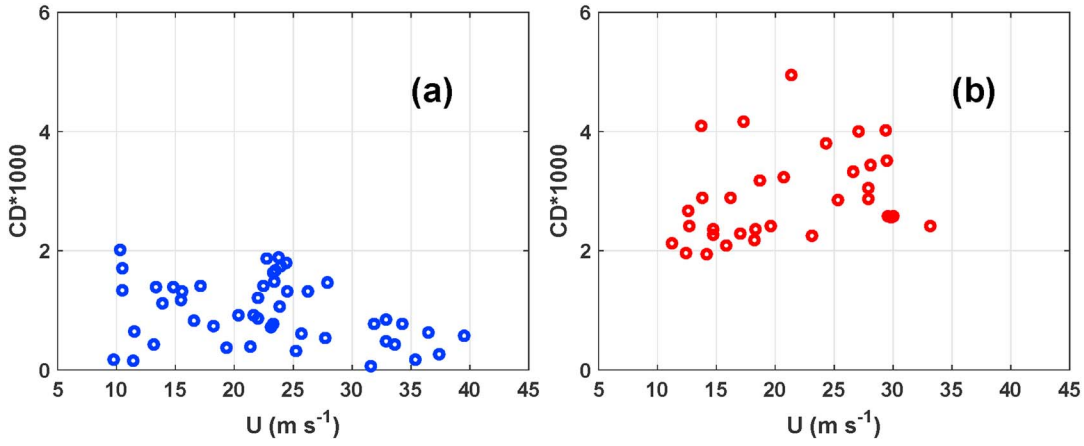

Figure 9. Plots of the drag coefficients as function of the mean wind speed for each flux run in (a) Typhoon Hagupit (2008, blue) and (b) Typhoon Chanthu (2010, red).

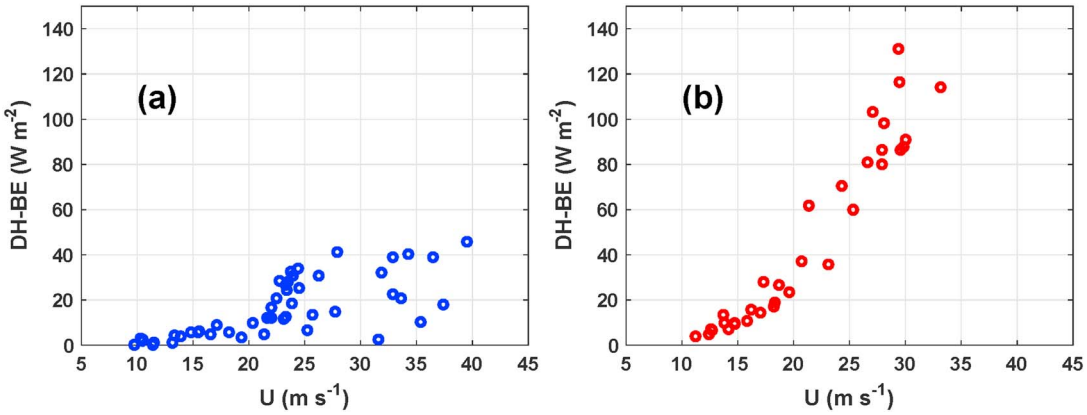

Figure 10. Plots of the DH calculated by the BE method as function of the mean wind speed for each flux run in (a) Typhoon Hagupit (2008, blue) and (b) Typhoon Chanthu (2010, red). DH = dissipative heating; BE = Bister and Emanuel.

the surface roughness. The values of C_D in Typhoon Chanthu (2010) varies from 0.002 to 0.006, which are close to those reported by Zhang, Zhu, et al. (2011) in landfalling hurricanes in which their observational towers were deployed inland and at locations with similar land surface types as Tower2. On the other hand, the values of the drag coefficient in Typhoon Hagupit (2008) are close to those reported by previous studies over the ocean (e.g., Bell et al., 2012; French et al., 2007; Powell et al., 2003). Over the open ocean, the drag coefficient is usually found to increase with wind speed when the wind speed is $<$25 m/s (e.g., Black et al., 2007; Donelan et al., 2004; Fairall et al., 1996; French et al., 2007; Large & Pond 1981; Smith, 1980). However, here we show that the drag coefficient during the landfall of Typhoon Hagupit (2008) is nearly independent of the wind speed for wind speed $<$25 m/s when the data were collected over an island that is surrounded by shallow water. There is a tendency for the drag coefficient to decrease with the wind speed when the wind speed is $>$25 m/s, which is similar to the result of Powell et al. (2003).

The DH was calculated using both the BE method and the turbulent spectra method for all the good flux runs in the two typhoons. Figure 10 shows the DH computed based on the BE method as a function of the wind speed. It is evident that the variation of the DH with the wind speed is similar to that of the momentum flux in both typhoons. Overall, there is a tendency for the DH to increase with the wind speed, which is in agreement with previous studies (Bister & Emanuel, 1998; Zhang, 2010; Zhang, Zhu, et al., 2011). In Typhoon Chanthu (2010), the DH increases with the wind speed much faster than that in Typhoon Hagupit (2008). For the wind speed $>$25 m/s, the magnitude of the DH in Typhoon Chanthu (2010) is nearly twice that in Typhoon Hagupit (2008), suggesting that DH varies with surface roughness for a given wind speed.

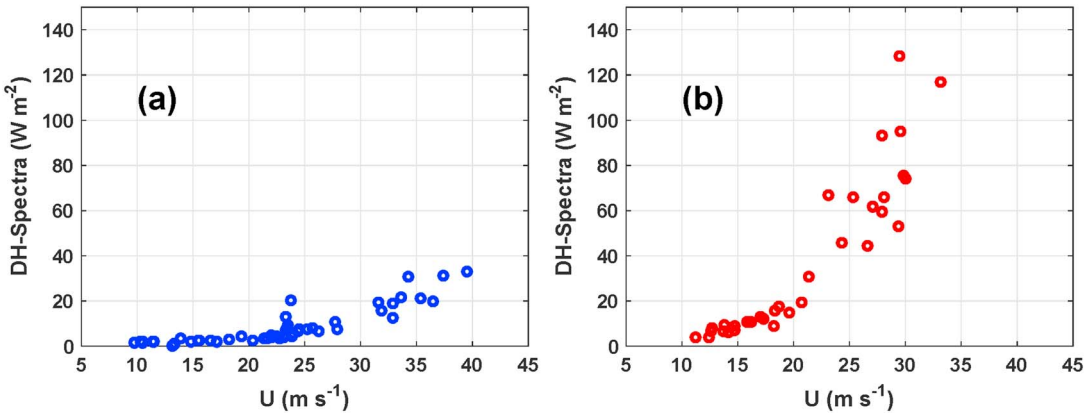

Figure 11. Plots of the DH calculated by the turbulent spectra method as function of the mean wind speed for each flux run in (a) Typhoon Hagupit (2008, blue) and (b) Typhoon Chanthu (2010, red). DH = dissipative heating.

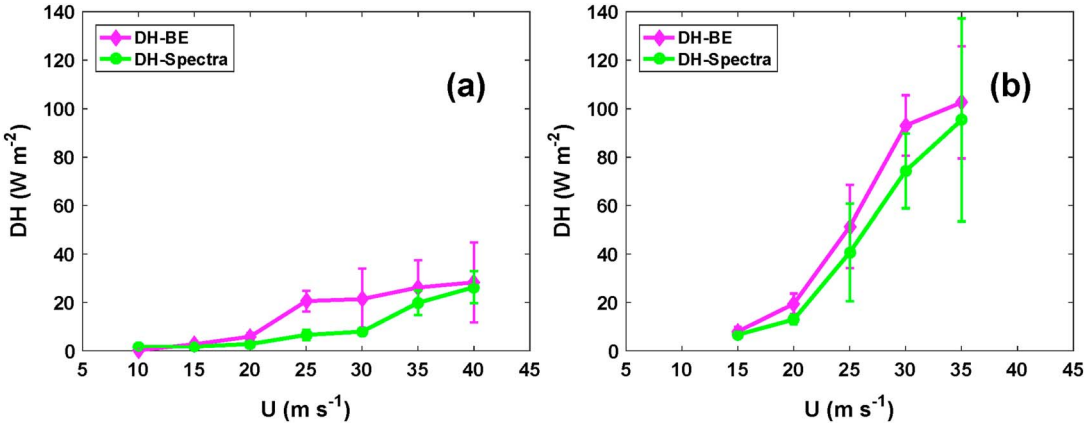

Figure 12. The bin-averaged DH estimated from the BE method (magenta) and the turbulent spectra method (green) plotted as function of the mean wind speed in: (a) Typhoon Hagupit (2008) and (b) Typhoon Chanthu (2010). The error bars represent the 95% confidence interval. DH = dissipative heating; BE = Bister and Emanuel.

Figure 11 shows the DH computed using the turbulent spectra method as a function of the wind speed, indicating a nearly continuous increase of the DH with the wind speed for both typhoons. Again, the magnitude of the DH in Typhoon Chanthu (2010) is much larger than that in Typhoon Hagupit (2008), in agreement with the behavior of the DH computed using the BE method.

Plotting the bin-averaged DH from both methods as a function of the wind speed in Figure 12 shows that the DH based on the BE method is generally larger than that based on the turbulent spectra method for both typhoons, in agreement with the findings of Zhang (2010) and Zhang, Zhu, et al. (2011). In Typhoon Hagupit (2008), the DH calculated by the BE method increases with the mean wind speed up to 25 m/s, and then tends to roll off for the wind speed $>$25 m/s, while the DH calculated by the turbulent spectra method increases slowly with the mean wind speed for the whole range of mean wind speed. In Typhoon Chanthu (2010), the DH calculated using the two methods behaves similarly, showing a monotonic increase of the DH with the wind speed. Statistical analysis shows that the difference in the DH estimated by the two methods is significant at 95% confidence interval only in Typhoon Hagupit (2008) for wind speed range between 25 and 35 m/s. There is no statistically significant difference in the DH estimated based on the two methods in Typhoon Chanthu (2010) at 95% confidence level. The difference is statistically significant only at the 75% confidence level.

Comparing the DH between the two methods for each flux run in a scatter plot (Figure 13) further confirms the result of the bin averages shown in Figure 12, in that the BE method overestimates the DH compared to

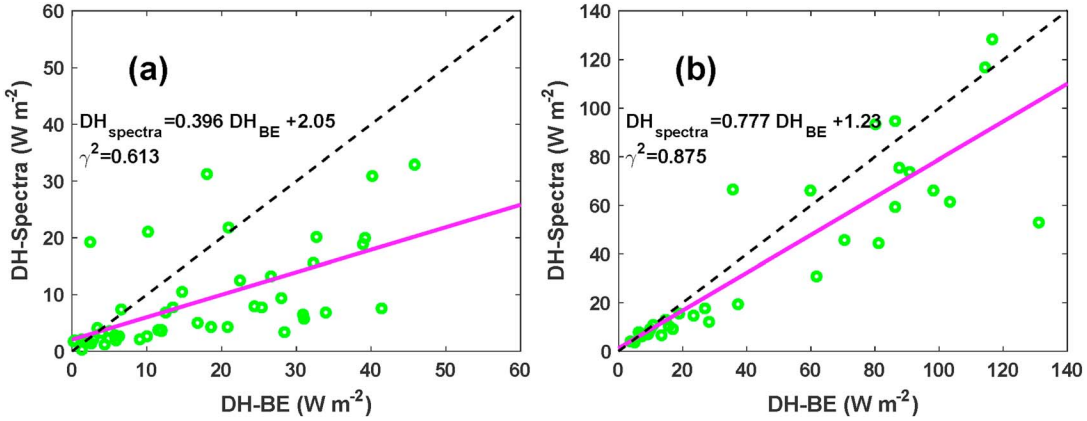

Figure 13. Comparisons of DH estimated by the BE method and the turbulent spectra method in: (a) Typhoon Hagupit (2008) and (b) Typhoon Chanthu (2010). The black dashed lines stand for the radio of 1:1 and the magenta solid lines stand for the least squares best fit between the data calculated by the two methods. The linear regression equations and correlation coefficients are also shown. DH = dissipative heating; BE = Bister and Emanuel.

the turbulent spectra method. The difference can be illustrated by the least squares best fit, with regression equations: $DH_{spectra} = 0.396\ DH_{BE} + 2.05$ for Typhoon Hagupit (2008), and $DH_{spectra} = 0.777\ DH_{BE} + 1.23$ for Typhoon Chanthu (2010), with 61.3% and 87.5% variance explained by the fitting equation. This result suggests that the difference in the DH estimated by the two methods becomes smaller when the storm is closer to land and the surface roughness is larger.

4. Discussion and Conclusion

In this paper, the high-frequency wind data, which were collected by two meteorology towers during TC landfalls, were analyzed to investigate the characteristics of the momentum flux, TKE, drag coefficient, roughness length, and DH with the different underlying surface conditions. Tower1 deployed in Typhoon Hagupit (2008) was located in a stand-alone small island where the surface roughness length is small as the tower is surround by sands and weeds and is close to the shallow water. Tower2 deployed in Typhoon Chanthu (2010) was located further inland from the coast where the surface roughness length is relatively large, as the upstream terrain types include farms, trees, and buildings. Both similarity and difference in the turbulence characteristics were observed by Tower1 and Tower2 during TC landfalls.

As expected, both towers observed the increase of the momentum flux and TKE with the wind speed, consistent with previous observational studies (e.g., Black et al., 2007; French et al., 2007; Ming et al., 2014; Potter et al., 2015; Tang et al., 2015). The DH measured by both towers is found to increase with the wind speed as well, in agreement with previous aircraft observations given by Zhang (2010) and tower observations given by Zhang, Zhu, et al. (2011).

With different underlying surface conditions, the measured magnitudes of the momentum flux and TKE by the two towers are different at the same given wind speed. When the surface is rougher around Tower2 in Typhoon Chanthu (2010), the measured momentum flux and TKE are substantially larger than those measured by Tower1 in Typhoon Hagupit (2008). When the wind speed is $>$25 m/s, the momentum flux tends to level off in shallow water condition (i.e., Tower1). The derived drag coefficient based on the direct flux measurement is also significantly different in terms of its magnitude from observations of Tower1 and Tower2. The drag coefficient measured by Tower2 over land is nearly twice that measured by Tower1 over the shallow water. No wind speed dependence of the drag coefficient is observed by the two towers, which is in agreement with land-based observations of the drag coefficient in moderate wind conditions (e.g., Mahrt et al., 2001). Tower1 measured a weak tendency for the drag coefficient to decrease with the wind speed when the wind speed is $>$25 m/s, which is similar to the results suggested by Powell et al. (2003).

The DH was estimated using two different methods following Zhang (2010): (1) the BE method and (2) the turbulent spectra method. Our result confirms that the DH generally increases with the wind speed based on estimates from both methods. In agreement with Zhang (2010) and Zhang, Zhu, et al. (2011), our analysis confirms that the BE method tends to overestimate the magnitude of DH compared to the turbulent spectra method that is more accurate based on direct turbulence observations. Interestingly, the overestimation of the DH by the BE method is found to be much smaller over land than over the shallow water. When the surface roughness is larger over land, the magnitude of the DH is also larger than that over shallow water. Zhang (2010) found that the BE method significantly overestimates the magnitude of the DH over the open ocean and attributed this overestimation to the energy dissipation by ocean waves. Our result supports this hypothesis as we found that the overestimation of the DH by the BE method becomes smaller and smaller as the observations are taken closer to the land. Without surface waves existing over land, all the energy caused by frictional dissipation could be turned to heat, so that the DH estimated by the BE method based on drag coefficient becomes consistent with the spectra method.

In the end, we note that the magnitude of the DH is as large as 100 W/m^2 above the hurricane force winds. This amount of energy is close to that from the sensible heat flux typically measured over the ocean (e.g., Zhang et al., 2008, 2013), suggesting that this energy from the DH cannot be neglected in numerical simulations and forecasts of landfalling TCs. In numerical models, when DH is included in the surface layer parameterization (i.e., the temperature tendency equation), we recommend to use the spectra method instead of the BE method. The DH can be computed by integrating the dissipation rate in the surface layer following equation (9) and the dissipation rate can be approximately estimated using the shear production

term over land. Over the ocean, a reduction (10%–30%) of shear production term should be considered to take into account the energy loss due to surface waves and ocean coupling processes.

Acknowledgments
This work was primarily supported by the National Natural Science Foundation of China (grants 41575044, 41575130, and 41675021), and National Fundamental Research 973 Program of China (2015CB452801). Jun Zhang was supported by NOAA's Hurricane Forecast Improvement project with award NA14NWS4680028, and National Science Foundation award AGS1822128. The authors are grateful to Lili Song for providing the observed data of Typhoon Hagupit (2008). The observed data used in this paper are available on ftp://114.212.52.5:2/. The username is datajgr and the password is datajgr.

References

Bell, M. M., Montgomery, M. T., & Emanuel, K. A. (2012). Air-sea enthalpy and momentum exchange at major hurricane wind speeds observed during CBLAST. *Journal of the Atmospheric Sciences*, *69*(11), 3197–3222. https://doi.org/10.1175/JAS-D-11-0276.1

Bender, M. A., Ginis, I., Tuleya, R., Thomas, B., & Marchok, T. (2007). The operational GFDL coupled hurricane–ocean prediction system and a summary of its performance. *Monthly Weather Review*, *135*(12), 3965–3989. https://doi.org/10.1175/2007MWR2032.1

Bister, M., & Emanuel, K. A. (1998). Dissipative heating and hurricane intensity. *Meteorology and Atmospheric Physics*, *65*(3-4), 233–240. https://doi.org/10.1007/BF01030791

Black, P. G., D'Asaro, E. A., Sanford, T. B., Drennan, W. M., Zhang, A. J., French, J. R., et al. (2007). Air-sea exchange in hurricanes: Synthesis of observations from the coupled boundary layer air-sea transfer experiment. *Bulletin of the American Meteorological Society*, *88*(3), 357–374. https://doi.org/10.1175/BAMS-88-3-357

Braun, S. A., & Tao, W.-K. (2000). Sensitivity of high-resolution simulations of Hurricane Bob (1991) to planetary boundary layer parameterizations. *Monthly Weather Review*, *128*(12), 3941–3961. https://doi.org/10.1175/1520-0493(2000)129%3C3941:SOHRSO%3E2.0.CO;2

Bryan, G. H. (2012). Effects of surface exchange coefficients and turbulence length scales on the intensity and structure of numerically simulated hurricanes. *Monthly Weather Review*, *140*(4), 1125–1143. https://doi.org/10.1175/MWR-D-11-00231.1

Businger, S., & Businger, J. (2001). Viscous dissipation of turbulence kinetic energy in storms. *Journal of the Atmospheric Sciences*, *58*(24), 3793–3796. https://doi.org/10.1175/1520-0469(2001)058%3C3793:VDOTKE%3E2.0.CO;2

Cheng, X. P., Fei, J. F., Huang, X. G., & Zheng, J. (2012). Effects of sea spray evaporation and dissipative heating on intensity and structure of tropical cyclone. *Advances in Atmospheric Sciences*, *29*(4), 810–822. https://doi.org/10.1007/s00376-012-1082-3

Davis, C., Wang, W., Chen, S. S., Chen, Y., Corbosiero, K., DeMaria, M., et al. (2008). Prediction of landfalling hurricanes with the advanced hurricane WRF model. *Monthly Weather Review*, *136*(6), 1990–2005. https://doi.org/10.1175/2007MWR2085.1

Donelan, M. A., Haus, B. K., Reul, N., Plant, W. J., Stiassnie, M., Graber, H. C., et al. (2004). On the limiting aerodynamic roughness of the ocean in very strong wind. *Geophysical Research Letters*, *31*, L18306. https://doi.org/10.1029/2004GL019460

Emanuel, K. A. (1986). An air–sea interaction theory for tropical cyclones. Part I: Steady-state maintenance. *Journal of the Atmospheric Sciences*, *43*(6), 585–605. https://doi.org/10.1175/1520-0469(1986)043%3C0585:AASITF%3E2.0.CO;2

Emanuel, K. A. (1995). Sensitivity of tropical cyclones to surface exchange coefficients and a revised steady-state model incorporating eye dynamics. *Journal of the Atmospheric Sciences*, *52*(22), 3969–3976. https://doi.org/10.1175/1520-0469(1995)052%3C3969:SOTCTS%3E2.0.CO;2

Fairall, C. W., Bradley, E. F., Rogers, D. P., Edson, J. B., & Young, G. S. (1996). Bulk parameterization of air-sea fluxes for tropical ocean-global atmosphere coupled-ocean atmosphere response experiment. *Journal of Geophysical Research*, *101*(C2), 3747–3764. https://doi.org/10.1029/95JC03205

French, J. R., Drennan, W. M., Zhang, J. A., & Black, P. G. (2007). Turbulent fluxes in the hurricane boundary layer. Part I: Momentum flux. *Journal of the Atmospheric Sciences*, *64*(4), 1089–1102. https://doi.org/10.1175/JAS3887.1

Green, B. W., & Zhang, F. (2014). Sensitivity of tropical cyclone simulations to parametric uncertainties in air–sea fluxes and implications for parameter estimation. *Monthly Weather Review*, *142*(6), 2290–2308. https://doi.org/10.1175/MWR-D-13-00208.1

Jin, Y., Thompson, W. T., Wang, S., & Liou, C.-S. (2007). A numerical study of the effect of dissipative heating on tropical cyclone intensity. *Weather and Forecasting*, *22*(5), 950–966. https://doi.org/10.1175/WAF1028.1

Kepert, J. D. (2012). Choosing a boundary layer parameterization for tropical cyclone modeling. *Monthly Weather Review*, *140*(5), 1427–1445. https://doi.org/10.1175/MWR-D-11-00217.1

Kieu, C. Q. (2015). Revisit dissipative heating in tropical cyclone maximum potential intensity. *Quarterly Journal of the Royal Meteorological Society*, *141*, 2497–2504. https://doi.org/10.1002/qj.2534

Large, W. G., & Pond, S. (1981). Open ocean momentum flux measurements in moderate to strong winds. *Journal of Physical Oceanography*, *11*(3), 324–336. https://doi.org/10.1175/1520-0485(1981)011%3C0324:OOMFMI%3E2.0.CO;2

Mahrt, L., Vickers, D., Sun, J., Jensen, N. O., Jørgensen, H., Pardyjak, E., & Fernando, H. (2001). Determination of the surface drag coefficient. *Boundary-Layer Meteorology*, *99*(2), 249–276. https://doi.org/10.1023/A:1018915228170

Malkus, J. S., & Riehl, H. (1960). On the dynamics and energy transformations in steady-state hurricanes. *Tellus*, *12*, 1–20.

Ming, J., & Zhang, J. A. (2016). Effects of surface flux parameterization on the numerically simulated intensity and structure of Typhoon Morakot (2009). *Advances in Atmospheric Sciences*, *33*(1), 58–72. https://doi.org/10.1007/s00376-015-4202-z

Ming, J., Zhang, J. A., Rogers, R. F., Marks, F. D., Wang, Y., & Cai, N. (2014). Multiplatform observations of boundary layer structure in the outer rainbands of landfalling typhoons. *Journal of Geophysical Research*, *119*, 7799–7814. https://doi.org/10.1002/2014JD021637

Nolan, D. S., Stern, D. P., & Zhang, J. A. (2009). Evaluation of planetary boundary layer parameterizations in tropical cyclones by comparison of in-situ data and high-resolution simulations of Hurricane Isabel (2003). Part II: Inner core boundary layer and eyewall structure. *Monthly Weather Review*, *137*(11), 3675–3698. https://doi.org/10.1175/2009MWR2786.1

Ooyama, K. (1969). Numerical simulation of the life cycle of tropical cyclones. *Journal of the Atmospheric Sciences*, *26*(1), 3–40. https://doi.org/10.1175/1520-0469(1969)026%3C0003:NSOTLC%3E2.0.CO;2

Potter, H., Graber, H. C., Williams, N. J., Collins, C. O., Ramos, R. J., & Drennan, W. M. (2015). In situ measurements of momentum fluxes in typhoons. *Journal of the Atmospheric Sciences*, *72*(1), 104–118. https://doi.org/10.1175/JAS-D-14-0025.1

Powell, M. D., Vickery, P. J., & Reinhold, T. A. (2003). Reduced drag coefficient for high wind speeds in tropical cyclones. *Nature*, *422*(6929), 279–283. https://doi.org/10.1038/nature01481

Smith, S. D. (1980). Wind stress and heat flux over the ocean in gale force winds. *Journal of Physical Oceanography*, *10*(5), 709–726. https://doi.org/10.1175/1520-0485(1980)010%3C0709:WSAHFO%3E2.0.CO;2

Smith, R. K., & Thomsen, G. L. (2010). Dependence of tropical-cyclone intensification on the boundary layer representation in a numerical model. *Quarterly Journal of the Royal Meteorological Society*, *136*(652), 1671–1685. https://doi.org/10.1002/qj.687

Sreenivasan, K. R. (1995). On the universality of the Kolmogorov constant. *Physics of Fluids*, *7*(11), 2778–2784. https://doi.org/10.1063/1.868656

Tang, J., Byrne, D., Zhang, J. A., Wang, Y., Lei, X., Wu, D., et al. (2015). Horizontal transition of turbulent cascade in the near-surface layer of tropical cyclones. *Journal of the Atmospheric Sciences*, *72*(12), 4915–4925. https://doi.org/10.1175/JAS-D-14-0373.1

Wang, Y. (2001). An explicit simulation of tropical cyclones with a triply nested movable mesh primitive equation model— TCM3. Part I: Description of the model and control experiment. *Monthly Weather Review*, *129*(6), 1370–1394. https://doi.org/10.1175/1520-0493(2001)129%3C1370:AESOTC%3E2.0.CO;2

Wroe, D. R., & Barnes, G. M. (2003). Inflow layer energetics of Hurricane Bonnie (1998) near landfall. *Monthly Weather Review*, *131*(8), 1600–1612. https://doi.org/10.1175//2547.1

Zeng, Z. H., Wang, Y. Q., Duan, Y. H., Chen, L. S., & Gao, Z. Q. (2010). On sea surface roughness parameterization and its effect on tropical cyclone structure and intensity. *Advances in Atmospheric Sciences*, *27*(2), 337–355. https://doi.org/10.1007/s00376-009-8209-1

Zhang, J. A. (2010). Estimation of dissipative heating using low level in situ aircraft observations in the hurricane boundary layer. *Journal of the Atmospheric Sciences*, *67*(6), 1853–1862. https://doi.org/10.1175/2010JAS3397.1

Zhang, D.-L., & Altshuler, E. (1999). The effects of dissipative heating on hurricane intensity. *Monthly Weather Review*, *127*(12), 3032–3038. https://doi.org/10.1175/1520-0493(1999)127%3C3032:TEODHO%3E2.0.CO;2

Zhang, J. A., Black, P. G., French, J. R., & Drennan, W. M. (2008). First direct measurements of enthalpy flux in the hurricane boundary layer: The CBLAST results. *Geophysical Research Letters*, *35*, L14813. https://doi.org/10.1029/2008GL034374

Zhang, J. A., Drennan, W. M., Black, P. G., & French, J. R. (2009). Turbulence structure of the hurricane boundary layer between the outer rainbands. *Journal of the Atmospheric Science*, *66*, 2455–2467. https://doi.org/10.1175/2009JAS2954.1

Zhang, J. A., Marks, F. D., Montgomery, M. T., & Lorsolo, S. (2011). An estimation of turbulent characteristics in the low-level region of intense Hurricanes Allen (1980) and Hugo (1989). *Monthly Weather Review*, *139*(5), 1447–1462. https://doi.org/10.1175/2010MWR3435.1

Zhang, J. A., Rogers, R. F., Reasor, P., Uhlhorn, E. W., & Marks, F. D. (2013). Asymmetric hurricane boundary layer structure from dropsonde composites in relation to the environmental vertical wind shear. *Monthly Weather Review*, *141*(11), 3968–3984. https://doi.org/10.1175/MWR-D-12-00335.1

Zhang, J. A., Zhu, P., Masters, F. J., Rogers, R. F., & Marks, F. D. (2011). On momentum transport and dissipative heating during hurricane landfalls. *Journal of the Atmospheric Sciences*, *68*(6), 1397–1404. https://doi.org/10.1175/JAS-D-10-05018.1